NJC

Accepted Manuscript

This article can be cited before page numbers have been issued, to do this please use: Y. Lai, C. Kao, Y. Chen, C. Fang, C. Hu and C. Chu, *New J. Chem.*, 2016, DOI: 10.1039/C5NJ03173G.

View Article Online
DOI: 10.1039/C5NJ03173G

Full Paper

Photodegradable Self-Assembling PAMAM Dendrons for Gene Delivery Involving Dendriplexes Formation and Phototriggered Circular DNA Release[†]

Yu-Sen Lai,[a] Chai-Lin Kao,[b] Ya-Pei Chen,[a] Chia-Chia Fang,[a] Chao-Chin Hu[a] and Chih-Chien Chu[a,c]

[a]Department of Medical Applied Chemistry, Chung Shan Medical University, Taichung 40201, Taiwan
[b]Department of Medical and Applied Chemistry, Kaohsiung Medical University, Kaohsiung 80708, Taiwan
[c]Department of Medical Education, Chung Shan Medical University Hospital, Taichung 40201, Taiwan

Correspondence to: Chih-Chien Chu; email: jrchu@csmu.edu.tw

[†]Electronic supplementary information (ESI) available: materials synthesis, NMR characterization, mass spectrometric data, particle size and zeta potential analysis. See DOI: XXX

View Article Online
DOI: 10.1039/C5NJ03173G

Abstract

For effective gene delivery, structural degradation of synthetic carriers is crucial to nucleic acids releasing on the transfection time scale. In this study, we have synthesized the amphiphilic dendritic scaffolds with a photolabile *o*-nitrobenzyl (*o*-NB) group that can enable the structural decomposition and controlled release of nucleic acids under active light stimulation. The amphiphilic counterpart composed of a lipophilic cholesterol and hydrophilic poly(amido amine) (PAMAM) dendron allows the self-assembly into a core-shell-like pseudodendrimer above the critical aggregation concentration (CAC) of approximately 20 μM. On the basis of electrostatic interaction, the polycationic pseudodendrimers is capable of forming stable complexes with polyanionic cyclic reporter gene under low charge excess value, suggesting substantial binding affinity of the dendron assembly toward circular DNA. Because the *o*-NB group in the dendritic structure undergoes efficient photolytic cleavage, in vitro test shows that thus-formed "dendriplexes" are readily dissociated under 365-nm light irradiation, causing effective dendron degradation accompanied by DNA release. This photochemical strategy provides an opportunity to control over the gene binding and releasing in a spatiotemporal manner.

Key words: amphiphilic dendrons; pseudodendrimer; photocage; nitrobenzyl; gene transfection

View Article Online
DOI: 10.1039/C5NJ03173G

Introduction

Dendrimers based on tailor-made surface functional groups and multivalent properties have been suggested as promising nanoscale synthetic carriers for delivering bioactive materials into target cells. An alternative to the processes required to prepare giant dendrimers with a well-defined hyperbranched structure, which are tedious and time-consuming, is using small amphiphilic dendron architectures in which a hydrophobic group at the focal point encourages self-assembly of the resulting amphiphilic dendrons into large "pseudodendrimers."[1-6] This supramolecular strategy, which enables combining polymer and lipid characteristics, can cause a synergistic effect, particularly in nucleic acid delivery. Recently, several studies have demonstrated remarkable DNA and small interfering RNA (siRNA) transfection in vitro and in vivo mediated by these amphiphilic dendrons.[7-10]

For effective gene delivery, synthetic carriers must overcome several extracellular and intracellular barriers including (1) nucleic acid complexation and protection, (2) cell membrane penetration, (3) endosomal escape, and (4) nucleic acid release for gene expression or knockdown.[11, 12] Principally, using the pseudodendrimers as gene vectors enables taking advantage of dynamic and responsive association and dissociation toward nucleic acids, which favors the encapsulation of nucleic acids through the multivalent ligand array assembled by the dendrons and rapid disassembly of these complexes under external stimuli (e.g., change in pH or ionic strength).[13, 14] To achieve the controlled release of nucleic acid after it enters the cells, complete dendron degradation has been suggested as mandatory for effective nucleic acid decomplexation. However, experimental and computer-aided simulation data have revealed that the structural degradation of the dendrons when bound to nucleic acids becomes ineffective on the transfection time scale, even at the lower pH associated with endosomes.[11] This key problem associated with barrier 4 on the transfection pathway makes gene delivery a challenging task, particularly for in vivo gene transfection.

View Article Online
DOI: 10.1039/C5NJ03173G

Recently, the concept of phototriggers has provided a useful strategy in photocontrolled drug delivery systems (PDDSs) because it enables rapid and accurate control over specific sites and times with external light stimulation.[15-20] Biologically relevant materials containing a photolabile building block can undergo efficient photolysis through active phototriggers, thus causing structural degradation and the release of biological targets. Among the numerous photolabile groups that have been studied, o-nitrobenzyl (*o*-NB) alcohol derivatives have aroused much attention in the PDDS field.[21-24] *o*-NB alcohol derivatives that undergo efficient photoisomerization are readily cleaved upon irradiation with UV light (approximately 300–350 nm) and then release a free carboxylic acid (COOH) and o-nitrosobenzaldehyde.[25] Because the *o*-NB group is highly sensitive to UV light, this photocleavage reaction can be induced within minutes, even when using a low-intensity light source. Moreover, simple chemical modifications to an aromatic ring enable tuning the absorption profiles of the *o*-NB group slightly. For example, an electron-donating substituent (e.g., OCH_3) functionalized at the para position of the NO_2 group can bathochromically shift the photocleavage wavelength to within the 350–400 nm range.

In this paper, we present amphiphilic dendritic scaffolds with a photolabile building block for creating photoresponsive pseudodendrimers that can enable the controlled release of nucleic acids under active light triggering. Generally, the amphiphilic structure composed of a hydrophilic poly(amido amine) (PAMAM) dendron and a lipophilic cholesterol molecule combines the advantageous gene delivery feature of lipid and polymer vectors. Furthermore, to overcome barrier 4, the cholesterol and dendron are interconnected by a photolabile *o*-NB group, enabling photoinduced degradation of the amphiphilic structure. Consequently, this strategy provides a remotely triggered route for accelerating nucleic acid release and enhancing gene transfection efficiency.[26] Aside from classical PAMAM dendrons, the novel dendron analogue that has inverse amide linkage to the amine branch are introduced for constructing the amphiphilic structures (Figure 1).[27]

View Article Online
DOI: 10.1039/C5NJ03173G

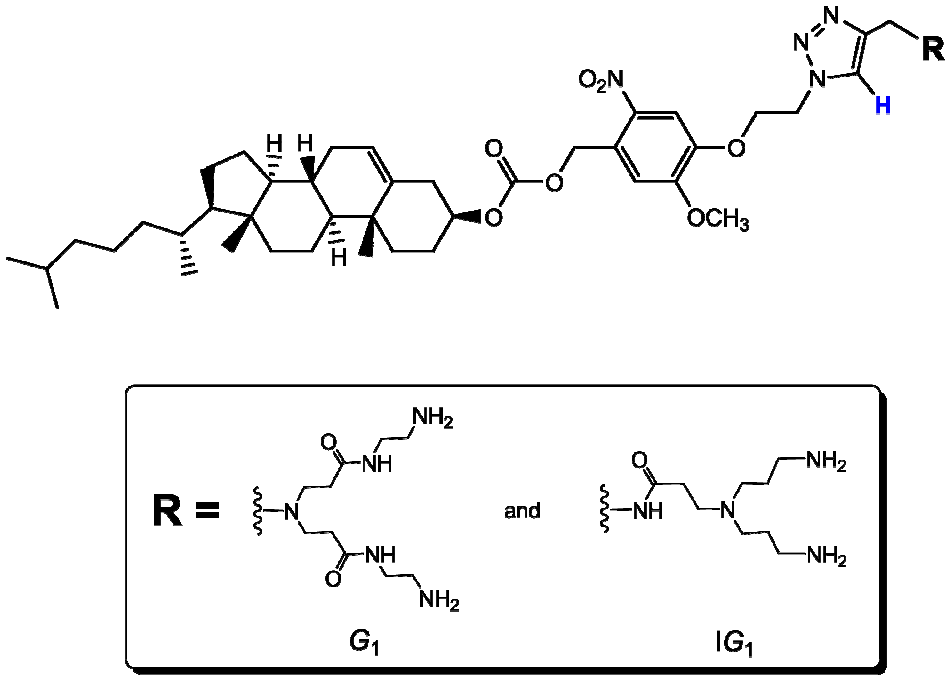

Figure 1. The o-nitrobenzyl (o-NB)-containing amphiphilic PAMAM dendrons. The H denote to characteristic triazole protons of the click clusters.

Results and discussion

Dendron synthesis and characterization

Figure 1 shows the classical PAMAM dendron and its analogue, namely G_1 and IG_1 respectively. G_1 dendron was synthesized through consecutive 1,4-Michael addition and amidation, with propargyl amine used as the starting material.[28] Moreover, IG_1 dendron with a COOH focal point was prepared using the synthetic method developed by Huang et al.[27] Carbodiimide-promoted amidation of IG_1 with propargyl amine yields the final propargyl-functionalized inverse dendrons. All amino groups of both dendrons were protected by the *tert*-butyloxycarbonyl (Boc) groups to prevent unwanted complexation of copper catalysts with NH_2 groups during the click reaction.

View Article Online
DOI: 10.1039/C5NJ03173G

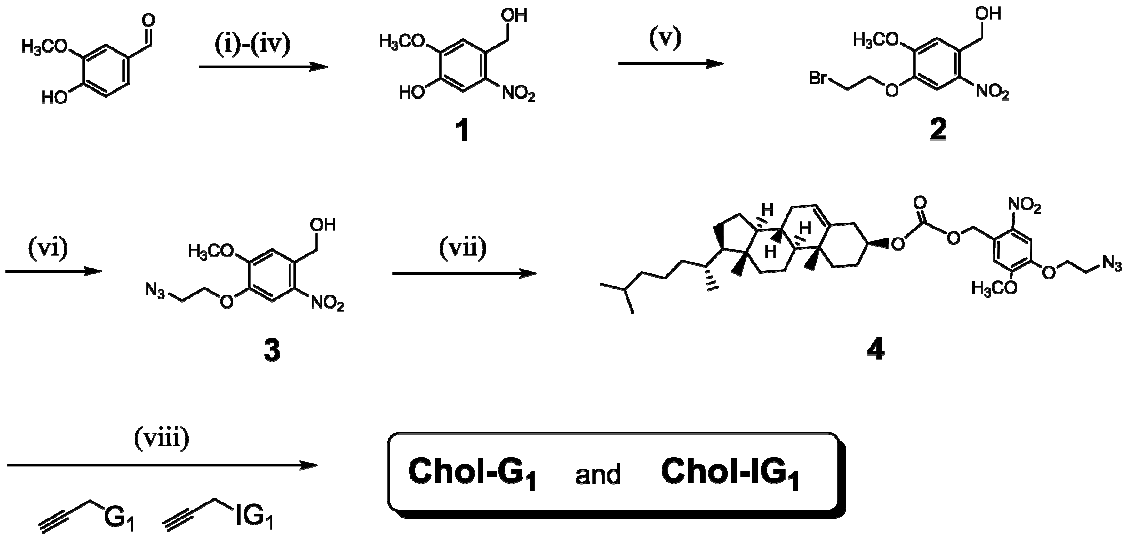

Scheme 1. Synthetic conditions: (i) Benzyl chloride, K_2CO_3, DMSO, 90°C; (ii) 65% HNO_3, CH_3COOH, ice bath to 25 °C; (iii) CF_3COOH, 25 °C; (iv) $NaBH_4$, EtOH, 25 °C; (v) 1,2-diboromoethane, K_2CO_3, 18-crown-6, THF, 40 °C; (vi) NaN_3, DMF, 90 °C; (vii) cholesteryl chloroformate, pyridine, THF, 40 °C; (viii) CuBr, THF, and then CF_3COOH, CH_2Cl_2, 25 °C.

As shown in Scheme 1, the *o*-NB alcohol derivative **1** was synthesized from commercially available vanillic aldehyde by following a modified procedure.[29] A nucleophilic substitution reaction at the phenolic proton yields compound **2**; following this with an azide substitution yields compound **3**. Subsequently, a simple esterification of **3** with cholesteryl chloroformate yields the precursor **4** with a carbonate linkage between the cholesterol and *o*-NB group. The terminal azide group enables "click" conjugation with propargyl-functionalized classical and inverse PAMAM dendrons through [3+2] copper-catalyzed azide-alkyne click reaction (CuAAC) protocols.[28] Finally, acid-promoted hydrolysis of the click products to remove the Boc protection yields the desired amphiphilic dendrons, namely **Chol-G_1** and **Chol-IG_1,** with photolabile *o*-NB building blocks.

Because the amphiphilic dendrons could exist in the form of giant aggregates rather than a single molecule in water or organic solvents, interpreting NMR spectra becomes a difficult task based on these complex resonance patterns of **Chol-G_1** and **Chol-IG_1** (see supporting information, Figure S3). Fortunately, successful click conjugation was readily confirmed

View Article Online
DOI: 10.1039/C5NJ03173G

according to the appearance of the triazole proton resonances at δ = 8.42 and 8.04 ppm, which correspond to the characteristic protons in the triazole linkages of **Chol-G_1** and **Chol-IG_1**, respectively (Figure 1). Moreover, the 1:1 integration ratio between the triazole proton and aromatic proton on the *o*-NB ring suggests effective CuAAC reaction of azide-terminated compound ***4*** with propargyl-functionalized G_1 or IG_1 dendron. More evidently, the absolute molecular weights for the amphiphilic dendrons were analyzed by performing MALDI-TOF-MS, with α-cyano-4-hydroxycinnamic acid used as a supporting matrix. The observed mass values were consistent with the calculated values of the protonated adducts of **Chol-G_1** and **Chol-IG_1** at 964.6 and 921.4 Da, respectively.

Self-assembly and photo-induced disassembly of dendrons

Because of the amphiphilic nature of a structure composed of a hydrophilic PAMAM dendron and a lipophilic cholesterol, **Chol-G_1** and **Chol-IG_1** assemble into Percec-type pseudodendrimers in an aqueous solution.[30] The structure of the pseudodendrimers is based on a core-shell-like micelle, in which the cholesterol aggregates are sheltered with PAMAM dendrons in aqueous media. The hydrophilic and lipophilic balance dominates the size, integrity, and morphology of the micelle-like pseudodendrimers. This self-assembly process was further confirmed using a Nile-red solubilization fluorescence assay, in which hydrophobic Nile-red dyes are used to observe the formation of a hydrophobic domain within an assembled nanostructure.[3, 31] Nile red is solubilized and emits appreciable orange-red fluorescence only when the dendron itself self-assembles into a micelle with a hydrophobic domain. Figure 2a,b shows that the self-assembly process was observed for **Chol-G_1** and **Chol-IG_1**, with discontinuity in the fluorescence intensity of Nile red at 635 nm plotted against increasing dendron concentration at the critical aggregation concentration (CAC). These results confirm that self-assembly occurs above the CAC. Using Nile-red assay, the CAC for **Chol-G_1** and **Chol-IG_1** in a phosphate buffer solution could be identified as

View Article Online
DOI: 10.1039/C5NJ03173G

approximately 20 μM, which is comparable to the CAC of cholesterol-based spermine dendrons.[1] In addition, we used dynamic light scattering (DLS) methods and assumed a spherical aggregation to further analyze the particle size of the self-assembled aggregates. The dimensions of **Chol-G_1** and **Chol-IG_1** aggregates formed in a phosphate buffer solution were approximately 114 ± 0.9 and 130 ± 1.4 nm, respectively.

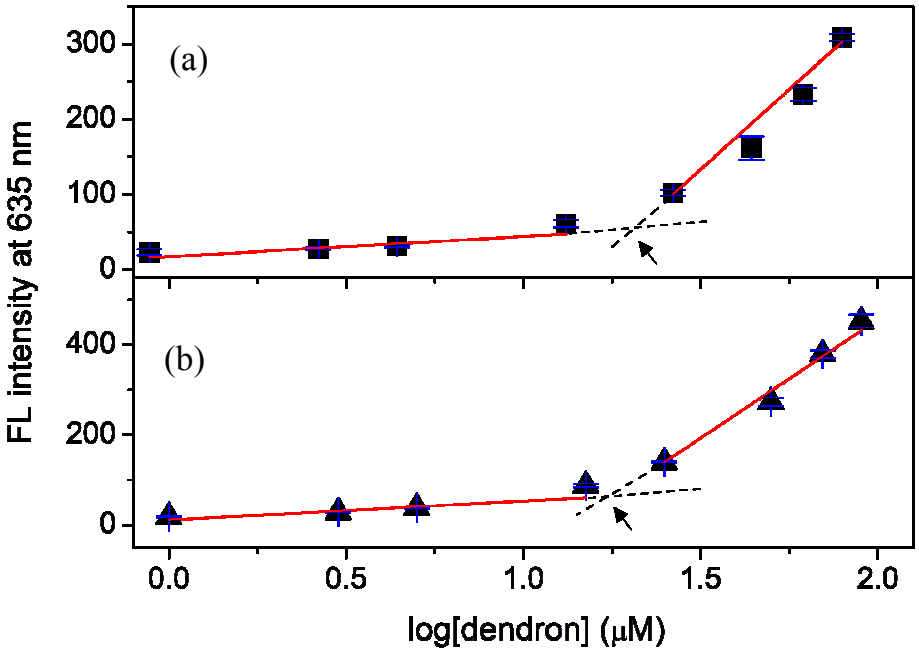

Figure 2. Fluorescence titration data of Nile-red solubilization assay to determine the critical aggregation concentration (CAC) of (a) **Chol-G_1** and (b) **Chol-IG_1** in a phosphate buffer solution (PBS, pH = 7.4). The CAC values are calculated by linear extrapolation of the linear regression fitting data.

Because the photocaged *o*-NB derivatives exhibit moderate absorption in the UV region, we examined the photoinduced degradation of the amphiphilic dendrons by using ultraviolet–visible (UV–Vis) spectroscopic analysis. The photocleavage reaction can be conducted under UV light; therefore, both dendron solutions were exposed to a 365-nm light-emitting diode (LED) at fixed time intervals (10, 20, and 30 min). Figure 3a,b illustrates the apparent changes in the absorption profiles of the **Chol-G_1** and **Chol-IG_1** solutions, respectively, upon UV light exposure. Furthermore, the **Chol-IG_1** dendron possesses observable red-shifted

View Article Online
DOI: 10.1039/C5NJ03173G

absorption bands in the UV region (300–400 nm). This result clearly suggests structural decomposition of the *o*-NB moiety from the original *o*-nitrobenzyl carbonate into *o*-nitrosobenzaldehyde after UV light irradiation.[32] Moreover, for both solutions, the appearance of a detectable absorption peak at 280 nm after light exposure indicates the formation of *o*-nitrosobenzaldehyde (see Figure S4).

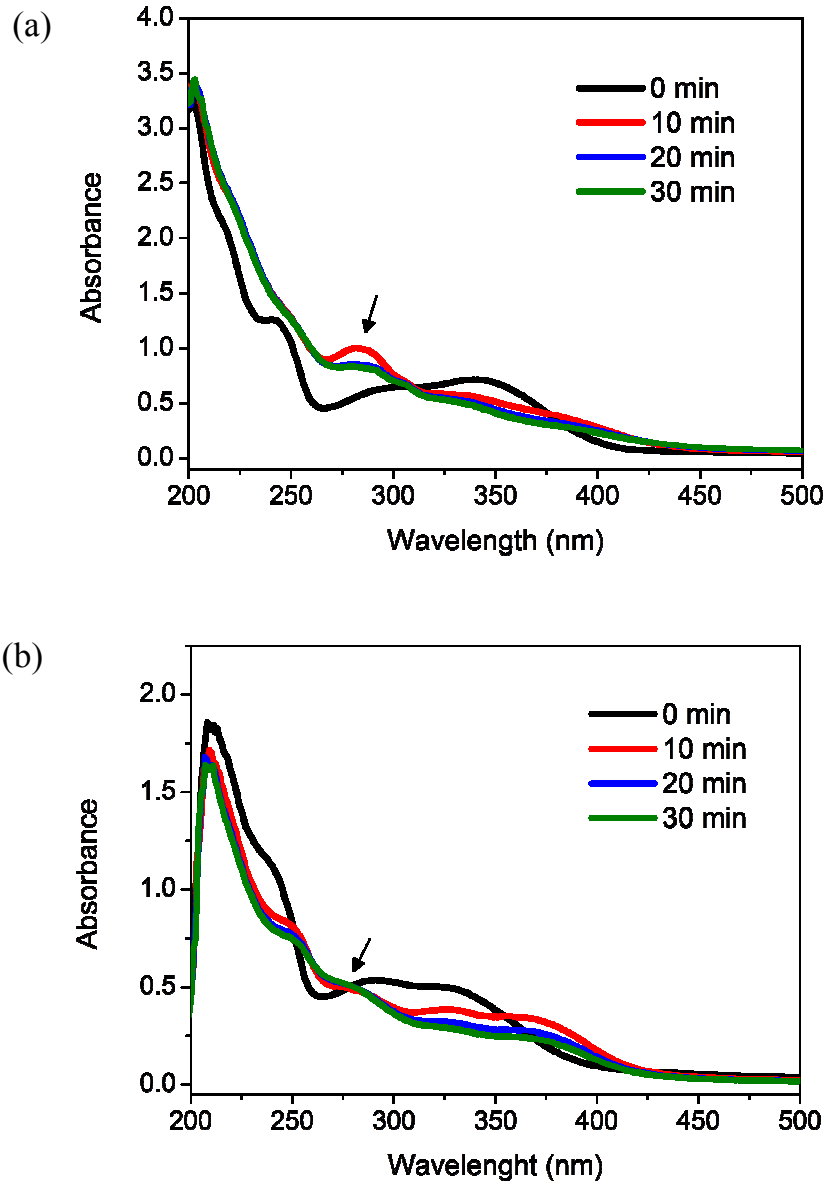

Figure 3. UV-Vis absorption spectra of (a) **Chol-G_1** and (b) **Chol-IG_1** aqueous solutions under 365-nm light-emitting diode (LED) irradiation. The appearance of absorption peak at 280 nm indicates successful photolysis of *o*-nitrobenzyl ester. The molar concentration for both dendron solutions is equal to 1 x 10^{-4} M.

View Article Online
DOI: 10.1039/C5NJ03173G

Because these amphiphilic dendrons undergo efficient photolytic structural degradation, dissociation of the self-assembly aggregates of the amphiphilic dendrons could also be activated by UV light trigger. The photoinduced disassembly process of **Chol-G_1** aggregates was then analyzed by the Nile-red assay. Notably, the concentration of the dendron solution was kept at 100 μM, which is fairly above the CAC, to ensure the micelle formation. As shown in Figure 4, the fluorescence intensity of Nile-red dramatically decreases and reaches a plateau after the solution was exposed to UV light for 20 min. This result suggests that the photocleavage of the *o*-NB groups could decompose the amphiphilic structure and thus causes the micelle deformation.

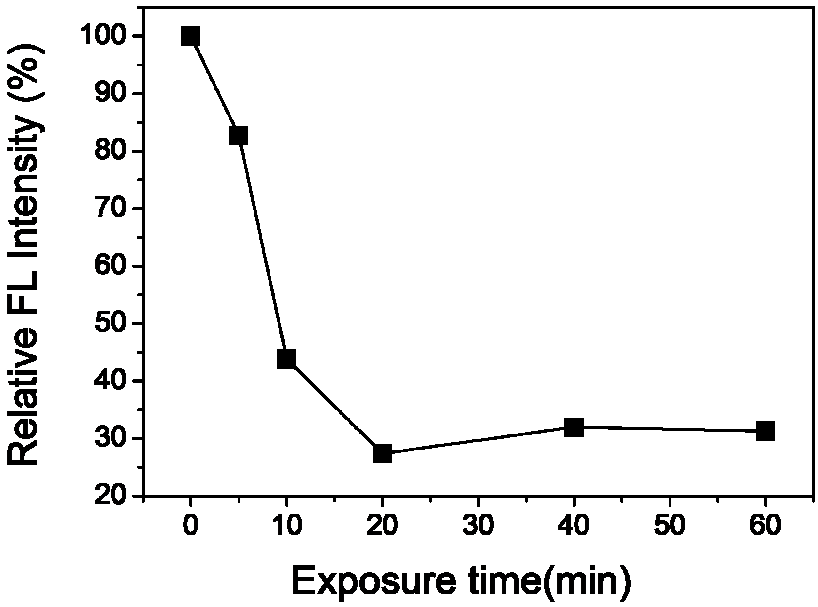

Figure 4. The relative fluorescence intensity of Nile-red in the presence of **Chol-G_1** (100 μM) after 365-nm light irradiation. The sample solutions were exposed to UV light at fixed time intervals, followed by adding the Nile-red probe to analyze the dendron assembly.

View Article Online
DOI: 10.1039/C5NJ03173G

DNA binding and photo-induced releasing

We then used the standard ethidium bromide (EtBr) displacement fluorescence spectroscopic assay to investigate the "dendriplexes" formation of these dendrons to bind pEGFP-C1 reporter DNA (approximately 4700 base pairs).[33, 34] This assay method involves using the competition between the DNA binder and EtBr to determine the concentration at which the DNA binder takes effect. This concentration can be expressed as a charge excess (CE_{50}) value, which reflects the concentration of the DNA binder required for half of the EtBr to be displaced from binding to DNA. This value is also the equivalent of a minimum nitrogen-to-phosphorus (N/P) ratio that is usually used to determine the amount of amine-based binding motifs required for effective DNA condensation through electrostatic interactions between the amine and phosphate groups. Initially, EtBr undergoes a large increase in fluorescence intensity upon intercalation with stacks of nucleic acid base pairs. The fluorometric titration experiments illustrated in Figure 5a,b reveal the fluorescence quenching of the EtBr/DNA complex in the presence of competing **Chol-G_1** and **Chol-IG_1**. This fluorescence quenching is due to the competitive displacement of EtBr by the amine-based dendrons.

View Article Online
DOI: 10.1039/C5NJ03173G

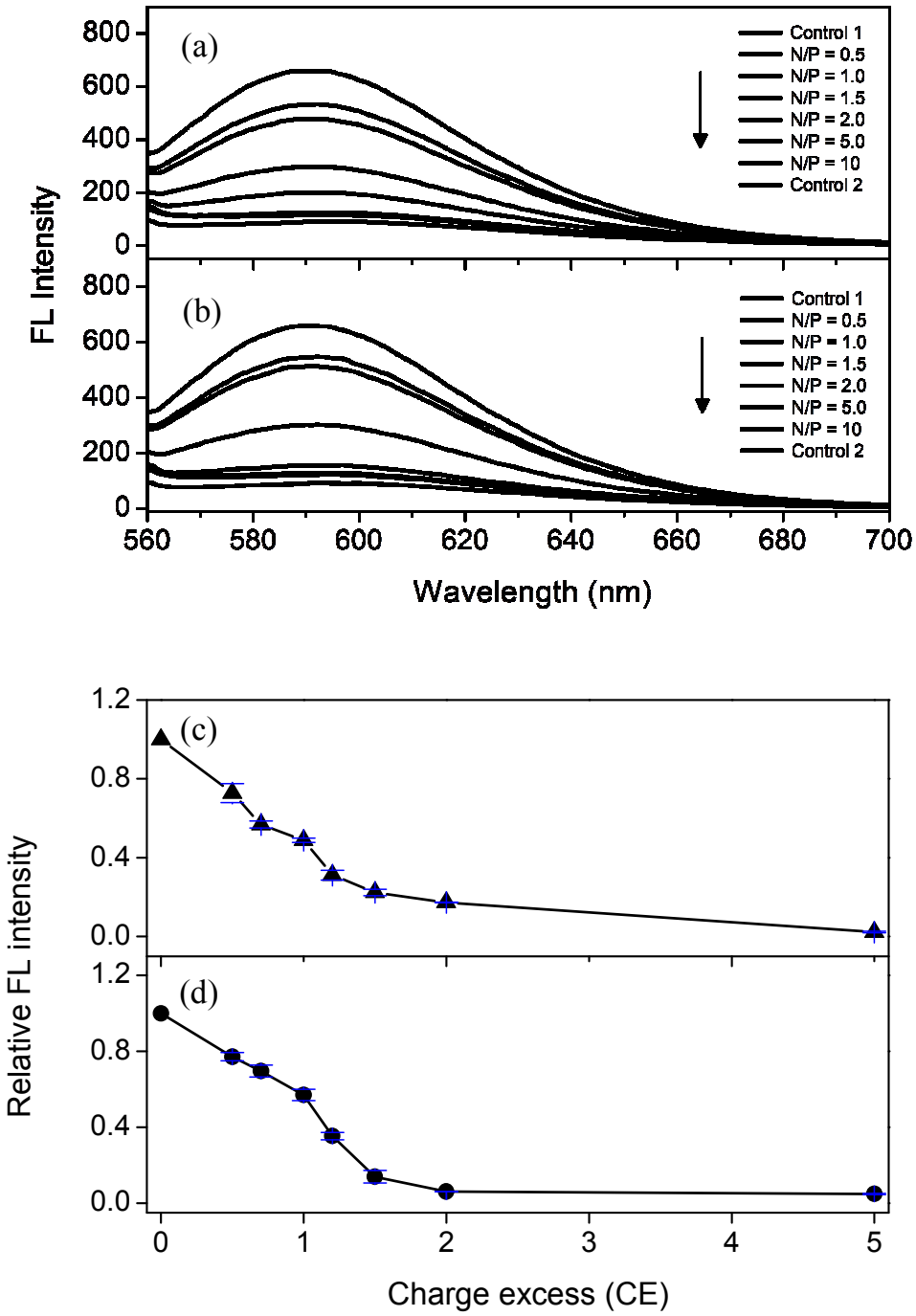

Figure 5. Fluorescence titration data of ethidum bromide (EtBr) displacement assay for addition of (a) **Chol-G_1** and (b) **Chol-IG_1** to pEGFP-C1 at increasing nitrogen-to-phosphorous (N/P) ratios. The control 1 corresponds to 1:1 binding of EtBr and a DNA base in the absence of dendrons, and the control 2 corresponds to the free EtBr in a phosphate buffer solution (PBS, pH = 7.4). The correlation of relative fluorescence intensity of EtBr at 590 nm versus the charge excess values of (c) **Chol-G_1** and (d) **Chol-IG_1** with DNA.

View Article Online
DOI: 10.1039/C5NJ03173G

Moreover, by maintaining the amounts of DNA (0.5 μg) and EtBr (0.7 μg) constant during all fluorometric assays, reduced fluorescence intensity was found to depend on the administered N/P values. As shown in Figure 5c,d, both amphiphilic dendrons possess similar DNA binding affinity, with calculated CE_{50} values of 0.92 and 0.97 for **Chol-*G*$_1$** and **Chol-I*G*$_1$**, respectively, indicating that 50% of the EtBr intercalated in the DNA could be successfully replaced by **Chol-*G*$_1$** and **Chol-I*G*$_1$** in phosphate buffer solutions. Accordingly, the minimum N/P ratio for effective DNA complexation is approximately equal to the CE_{50} values. We also performed a control experiment by using both ***G*$_1$** and **I*G*$_1$** dendrons as the DNA binder and found no fluorescent reduction at N/P ratio of 1. This result suggests that the amphiphilic structure containing cholesteryl and PAMAM dendritic counterparts is crucial for DNA complexation. DNA complexation was further analyzed by recording zeta potential measurements. The pristine pEGFP-C1 possesses a negative surface charge of approximately -54.7 ± 2.6 mV and was neutralized by adding **Chol-*G*$_1$** at an N/P ratio of 2. The surface potential shifted positively to +0.47 ± 0.1 mV, clearly confirming effective binding between DNA and the vectors above the CE_{50}.

The EtBr assay can also be used to study the UV-light-induced disassembly of the DNA and amphiphilic dendron complexes. We reasoned that as the dendrons degraded under UV light exposure, the DNA should be released and the EtBr is reintercalated into the double helix, thus reactivating its fluorescence. Before the test, two control experiments confirmed that (1) the DNA structure is insensitive to the 365-nm LED because the fluorescence intensity of the EtBr/DNA complex in the absence of amphiphilic dendrons remained at the highest value upon light exposure for 30 min, and (2) the fluorescence intensity remained essentially at the lowest value if the complex solution was maintained in the dark for 24 h in the presence of amphiphilic dendrons at an N/P ratio of 2. This result suggests that the DNA cannot be released from the electrostatic complexes because the amphiphilic dendrons possess an intact structure. The bar chart in Figure 6 indicates successful DNA release upon UV-light

View Article Online
DOI: 10.1039/C5NJ03173G

exposure. First, the fluorescence of EtBr at λ_{max} = 590 nm decreases because the EtBr is displaced from the DNA double helix by the presence of **Chol-*G*$_1$** and **Chol-I*G*$_1$** at an N/P ratio of 2. After UV light irradiation within 10 min, the clear increase in fluorescence intensity indicates disassembly of the DNA complexes. UV–Vis analysis demonstrated that both **Chol-*G*$_1$** and **Chol-I*G*$_1$** are highly sensitive to UV light, and thus the fluorescence enhancement is apparently due to EtBr reintercalation into DNA resulting from the photoinduced structural degradation of the amphiphilic dendrons that associates with DNA release. DLS measurement also supports the photoinduced dissociation of the DNA complexes. Initially, the dimensions of DNA–**Chol-*G*$_1$** complexes formed in an aqueous buffer solution were approximately 277 ± 57.3 nm; however, after light irradiation, hydrodynamic size distribution was undetectable by the DLS method, suggesting the disappearance of the DNA complexes. Moreover, zeta potential of the complex solution decreases from +0.47 ± 0.1 mV before irradiation to -44.6 ± 1.5 mV after irradiation. This negative shift of surface potential also confirms the phototriggered release of polyanionic DNA into surrounding solutions.

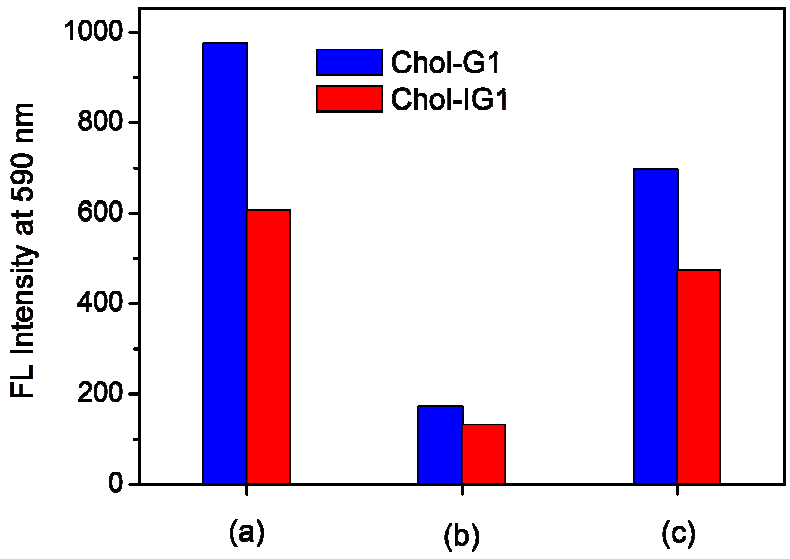

Figure 6. Fluorescence intensity of EtBr in the presence of (a) pEFGP-C1 and of (b) dendriplexes composed of pEGFP-C1/**Chol-*G*$_1$** or **Chol-I*G*$_1$** at N/P = 2. (c) The emission intensity was recovered after 365-nm light irradiation for 10 min, suggesting dendrons degradation and EtBr reintercalation into DNA.

View Article Online
DOI: 10.1039/C5NJ03173G

Barnard et al. argued that complete dendron degradation is necessary for effective DNA release.[11] However, when bound to DNA, dendron degradation becomes ineffective on a transfection-relevant time scale (hours). We supposed that is because DNA complexation may increase the stability of the dendrons against environmental fluctuation (e.g., the change in pH associated with endosomes). Because a photolabile *o*-NB building block exists in the dendrons, structural breakdown can be effectively triggered using UV light irradiation within several minutes, even in the presence of DNA. This photoinduction strategy enables DNA release on the transfection time scale under an actively triggered route. Moreover, by using water-soluble tetrazolium (WST) salt to assess metabolic cytotoxicity, **Chol-*G*$_1$** and **Chol-I*G*$_1$** were found to be nontoxic to the Smulow–Glikcman (SG) gingival cell lines at up to 100 μg/mL (Figure 7). The test indicated that high doses of both vectors do not induce a cytotoxic response. The efficiency of gene transfection has been suggested as usually being optimized with increasing N/P ratios, and thus the transfection can be conducted until an approximate N/P value of 50, which is substantially higher than the value for effective DNA binding. In vivo gene transfection facilitated by phototriggers toward SG cells by using the photoresponsive amphiphilic dendrons as synthetic vectors is currently under investigation.

View Article Online
DOI: 10.1039/C5NJ03173G

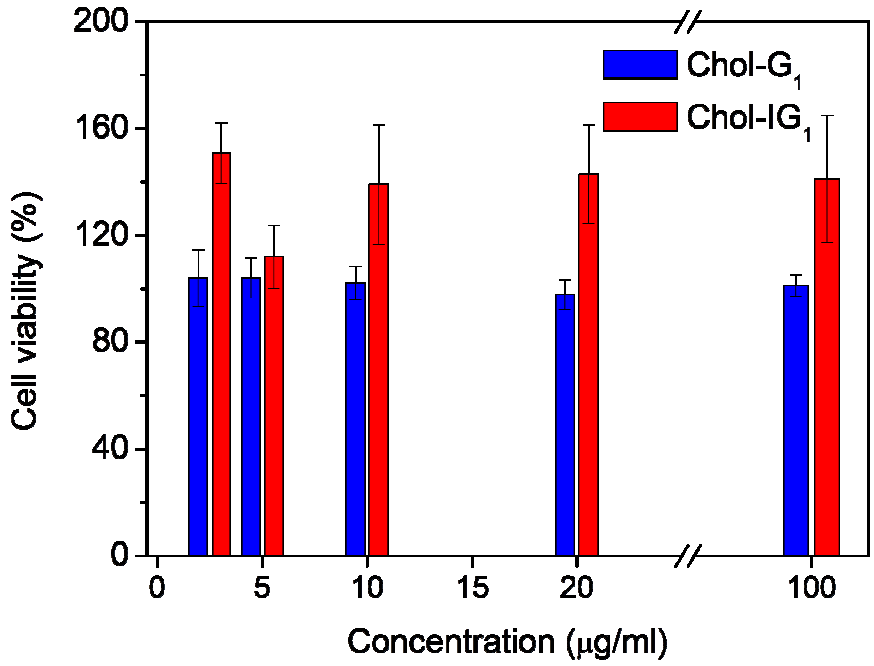

Figure 7. Smulow–Glikcman (SG) gingival cell viability test in the presence of **Chol-*G*$_1$** and **Chol-I*G*$_1$**.

Conclusion

In summary, we successfully synthesized photoresponsive amphiphilic PAMAM dendrons bearing photolabile *o*-NB building blocks as DNA carriers. Both amphiphilic dendrons comprising classical and inverse PAMAM dendritic scaffolds exhibit similar self-assembly behavior in the formation of micelle-like pseudodendrimers in an aqueous solution. On the basis of the bipolar functionality, **Chol-*G*$_1$** and **Chol-I*G*$_1$** also demonstrate substantial binding affinity with cyclic DNA at low N/P values. Most critically, thus-formed DNA complexes are readily dissociated under UV light irradiation because the *o*-NB group in the dendritic structure undergoes efficient photolytic cleavage, causing effective dendron degradation accompanied by DNA release. This photochemical strategy provides an opportunity to control over the gene binding and releasing in a spatiotemporal manner.

View Article Online
DOI: 10.1039/C5NJ03173G

Experimental section

Materials and instruments

All reagents were purchased as high-purity reagent-grade chemicals from either Sigma-Aldrich or Acros and used without further purification. The circular reporter DNA (pEGFP-C1) was a generous gift from Prof. Wen-Wei Chang. Classical poly(amido amine) (PAMAM) dendron (G_1) was synthesized via a divergent pathway,[28] and the dendron analogue (IG_1) was prepared by a solid-phase synthetic method.[27] All organic solvents for organic synthesis were distilled over suitable drying reagents under N_2 atmosphere before use. ^{1}H (400 MHz) and ^{13}C (75 MHz) NMR spectra were recorded on a Varian Mercury Plus 400 MHz spectrometer at room temperature using $CDCl_3$, DMSO-d_6, methanol-d_4, or D_2O as the solvents. Spectral processing (Fourier transform, peak assignment, and integration) was performed using MestReNova 6.2.1 software. Matrix-assisted laser desorption ionization/time-of-flight mass spectrometry (MALDI-TOF-MS) was performed on a Bruker AutoFlex III TOF/TOF system in positive ion mode using either 2,5-dihydroxybenzoic acid or α-cyano-4-hydroxycinnamic acid as the desorption matrix. The size and zeta potential measurements were recorded on a Horiba SZ-100 nanopartica series instrument using 532 nm laser as the incident light source. Ultraviolet-visible (UV-Vis) absorption spectra was performed on a Thermo Genesys 10S UV-Vis spectrometer. Fluorescence emission spectra was recorded on a Hitachi F-2500 spectrometer. Photolysis of the ester conjugates were carried out by using light-emitting diodes (LED) at 365 nm and an output power of 10-watt.

Synthesis of propargyl-functionalized IG_1

A CH_2Cl_2 solution (2 mL) of dicyclohexylcarbodiimide (DCC, 51 mg, 0.25 mmol) was added dropwise into a CH_2Cl_2 solution (3 mL) of IG_1 (50 mg, 0.12 mmol), propargylamine (40 μL, 0.62 mmol), and 1-hydroxybenzotriazole (5.1 mg, 10 wt % of DCC) under N_2 at 0 ^{o}C. After 15 min, the mixture was then stirred under room temperature for overnight. The reaction

View Article Online
DOI: 10.1039/C5NJ03173G

mixture was cooled to 0 °C to insure complete precipitation of the byproduct dicyclohexylurea, which is quickly removed by vacuum filtration. After rotatory evaporation to dryness, the crude product was further purified by flash column chromatography (SiO_2, ethyl acetate/hexane 2:3) to give propargyl-functionalized IG_1 as a colorless liquid (36 mg, 66%). ^{1}H-NMR (400 MHz, $CDCl_3$): δ = 4.95 (bs, 2H), 4.04 (dd, J = 5.1, 2.5 Hz, 2H), 3.16 (dd, J = 12.3, 6.2 Hz, 4H), 2.71 (t, J = 6.2 Hz, 2H), 2.46 (t, J = 6.6 Hz, 4H), 2.35 (t, J = 6.2 Hz, 2H), 2.22 (t, J = 2.5 Hz, 1H), 1.60-1.68 (m, 4H), 1.44 (s, 18H). ^{13}C-NMR (75 MHz, $CDCl_3$): δ = 172.4, 156.4, 80.2, 79.5, 71.4, 51.6, 50.9, 38.9, 33.9, 28.9, 28.7, 27.5.

Synthesis of (4-(2-bromoethoxy)-5-methoxy-2-nitrophenyl)methanol 2

4-(hydroxymethyl)-2-methoxy-5-nitrophenol ***1*** was synthesized from commercial available vanillin in 4 steps following a modified procedure (see supporting information).[29] To a tetrahydrofuran solution (THF, 25 mL) of ***1*** (1.35 g, 6.8 mmol), K_2CO_3 (0.88 g, 24 mmol), 18-crown-6 (2.7 g, 37 mmol), and 1,2-dibromoethane (3.5 g, 18 mmol) was added dropwise under N_2. After stirred at 40 °C for 4 h until the disappearance of the compound ***1***, the mixture was extracted by ethyl acetate/brine for 3 times. The combined organic phase was dried over anhydrous magnesium sulfate, and rotatory evaporation to dryness afforded compound ***2*** as pale-yellow solids (2.0 g, 96%). ^{1}H-NMR (400 MHz, $CDCl_3$): δ = 7.74 (s, 1H), 7.22 (s, 1H), 4.98 (d, *J* = 5.8 Hz, 2H), 4.52 (bs, 1H), 4.40 (t, *J* = 6.4 Hz, 2H), 4.00 (s, 3H), 3.70 (t, *J* = 6.4 Hz, 2H). ^{13}C-NMR (75 MHz, $CDCl_3$): δ = 154.8, 146.8, 139.7, 133.4, 111.6, 110.3, 68.6, 63.2, 56.7, 28.8.

Synthesis of (4-(2-azidoethoxy)-5-methoxy-2-nitrophenyl)methanol 3

A dimethylformamide solution (DMF, 20 mL) of ***2*** (0.53 g, 1.7 mmol) and NaN_3 (1.1 g, 17 mmol) was stirred at 90 °C for overnight under N_2. The solvent was removed under vacuum, and the mixture was extracted by ethyl acetate/brine for 3 times. The combined organic phase was dried over anhydrous magnesium sulfate, and rotatory evaporation to dryness afforded compound ***3*** as pale-yellow solids (0.32 g, 70%). ^{1}H-NMR (400 MHz, $CDCl_3$): δ = 7.73 (s,

View Article Online
DOI: 10.1039/C5NJ03173G

1H), 7.22 (s, 1H), 4.98 (bs, 2H), 4.52 (bs, 1H), 4.25 (t, *J* = 5.0 Hz, 2H), 4.00 (s, 3H), 3.69 (t, *J* = 5.0 Hz, 2H). ^{13}C-NMR (75 MHz, $CDCl_3$): δ = 154.8, 146.9, 139.7, 133.4, 111.6, 110.4, 68.6, 63.0, 56.7, 50.2.

Synthesis of Cholesterol-functionalized compound 4

A THF solution (10 mL) of ***3*** (0.10 g, 0.37 mmol), cholesteryl chloroformate (0.2 g, 0.45 mmol), and pyridine (46 μL, 0.57 mmol) was stirred at 40 ^{o}C for overnight under N_2. The solvent was removed under vacuum, and the crude product was purified by flash column chromatography (SiO_2, ethyl acetate/hexane 1:4) to give compound ***4*** as pale-yellow solids (0.13 g, 52%). ^{1}H-NMR (400 MHz, $CDCl_3$): δ = 7.75 (s, 1H), 7.08 (s, 1H), 5.58 (s, 2H), 5.41 (bs, 1H), 4.50-4.58 (m, 1H), 4.25 (t, *J* = 4.9 Hz, 2H), 3.98 (s, 3H), 3.70 (t, *J* = 4.9 Hz, 2H), 2.43 (bs, 2H), 0.85-2.03 (m, 38H), 0.68 (s, 3H). ^{13}C-NMR (75 MHz, $CDCl_3$): δ = 154.5, 154.3, 147.1, 139.5, 139.3, 128.3, 123.4, 110.4, 78.7, 68.6, 66.2, 56.9, 56.7, 56.3, 50.2, 42.5, 39.9, 39.7, 38.2, 37.1, 36.8, 36.4, 36.0, 32.1, 32.0, 28.5, 28.2, 27.9, 24.5, 24.1, 23.1, 22.8, 21.3, 19.5, 18.9, 12.1.

Synthesis of click clusters Chol-G_1 and Chol-IG_1

An anhydrous THF solution of compound **4** (21.0 mg, 30.8 μmol), Boc-protected ***G*$_1$** (18 mg, 37.2 μmol) or **I*G*$_1$** (17 mg, 38.6 μmol), and CuBr (5.3 mg, 36.9 μmol) was vigorously stirred at room temperature until the complete disappearance of compound **4**. The resulting solution was then extracted with ethyl acetate; the organic phase was washed with aqueous ammonia solution to remove copper catalyst and then dried over magnesium sulfate. Rotatory evaporating to dryness yields the Boc-protected click clusters quantitatively. For Boc-protected **Chol-*G*$_1$**, ^{1}H-NMR (400 MHz, $CDCl_3$): δ = 7.78 (s, 1H), 7.70 (s, 1H), 7.08 (s, 1H), 5.56 (s, 2H), 5.40 (bs, 1H), 4.85 (bs, 2H), 4.53 (m, 1H), 4.46 (bs, 2H), 3.97 (s, 3H), 3.40 (bs, 2H), 3.32 (bs, 4H), 3.23 (bs, 4H), 2.74 (bs, 4H), 2.42 (m, 6H), 0.85-2.05 (m, 56H), 0.68 (s, 3H); For Boc-protected **Chol-I*G*$_1$**, ^{1}H-NMR (400 MHz, $CDCl_3$): δ = 7.86 (s, 1H), 7.69 (s, 1H), 7.07 (s, 1H), 5.56 (s, 2H), 5.39 (bs, 1H), 4.80 (t, *J* = 5.0 Hz, 2H), 4.50-4.54 (m, 3H), 4.44 (t, *J*

View Article Online
DOI: 10.1039/C5NJ03173G

= 5.0 Hz, 2H), 3.97 (s, 3H), 3.08-3.16 (m, 4H), 2.68 (m, 2H), 2.43 (m, 6H), 2.35 (bs, 2H), 0.85-2.03 (m, 60H), 0.68 (s, 3H). Boc-deprotection is readily carried out by acid-promoted hydrolysis. Excess trifluoroacetic acid was added dropwise into an anhydrous CH_2Cl_2 solution of Boc-protected click clusters. The mixture was then stirred under room temperature for 3 days, and the volatiles were removed under reduced pressure. The mixture was rinsed with hexane repetitively to remove excess acid, and then freeze-drying afforded amphiphilic dendrons as yellowish fluffy powders (72% for **Chol-G_1**, 63% for **Chol-IG_1**). The NMR analysis is shown in the supporting information.

General methods for the photolysis and photorelease

The photolytic reaction was performed by irradiating the sample solutions prepared in a quartz cuvette (1 cm x 1 cm) under a 10-watt LED (365 nm). The distance between the sample and light source was kept at approximately 3 cm, and the exposed solutions were analyzed by either UV-Vis absorption or fluorescence spectroscopy.

Nile-red solubilization assay

A Nile red stock solution (2.5 mM) was prepared in ethanol, and a dendron stock solution was prepared in PBS buffer at various concentrations depending on the starting concentration for the assay. Aliquots of the stock solution were taken and diluted with PBS to the desired concentration in a 1 mL assay volume. Nile red (1 μL) was added and the fluorescence emission was measured on a spectrofluorometer using an excitation wavelength of 550 nm. Fluorescence intensity was recorded at 635 nm. Experiments were performed in triplicate.

EtBr displacement assay

0.5 mL of pEGFP-C1 solution (1 μg/mL) and 7 μL of EtBr solution (0.1 mg/mL) were mixed thoroughly in PBS buffer, followed by adding 8 μL of the dendron solutions to the desired N/P values. EtBr in ultrapure water was measured as the background fluorescence of EtBr, and the solution that only contains pEGFP-C1 and EtBr in 1:1 binding ratio corresponds to

View Article Online
DOI: 10.1039/C5NJ03173G

the N/P = 0 with maximum emission intensity. The fluorescence emission was measured on a spectrofluorometer using an excitation of 540 nm, and the emission spectra were recorded from 540 nm to 700 nm. Experiments were performed in triplicate.

WST cell proliferation assay

Prior to cytotoxicity measurement, SG cells were grown in 96-well plate at a density of 3×10^4 cells per well. After incubation for 24 h, dendron solutions were added into each well to attain the desired concentrations. After incubation at 37 ^oC for 48 h, a solution of 2-(4-iodophenyl)-3-(4-nitrophenyl)-5-(2,4-disulfophenyl)-2H-tetrazolium salt (WST-1) as 10 μL/well was added and the mixture was incubated at 37 ^oC for another 3 h. The viability of the cells was determined by visible absorbance at 440 nm after subtracting the reference absorbance at 650 nm with an ELISA microplate reader (EZ Read 400, Biochrom Ltd., Cambridge, UK). Four independent experiments were performed, and each experiment was done in triplicate.

Acknowledgements

The authors would like to thank Chung Shan Medical University and Ministry of Science and Technology (MOST) of Taiwan, for financially supporting this research (MOST103-2113-M-040-003). The authors are also grateful to Prof. Hsieh-Chih Tsai for support with size and zeta potential measurements and to Prof. Wen-Wei Chang for support with cytotoxicity test.

References

1. P. Posocco, S. Pricl, S. Jones, A. Barnard and D. K. Smith, *Chem. Sci.*, 2010, **1**, 393-404.
2. S. P. Jones, N. P. Gabrielson, C.-H. Wong, H.-F. Chow, D. W. Pack, P. Posocco, M. Fermeglia, S. Pricl and D. K. Smith, *Mol. Pharm.*, 2011, **8**, 416-429.
3. D. J. Welsh and D. K. Smith, *Org. Biomol. Chem.*, 2011, **9**, 4795-4801.
4. A. Barnard and D. K. Smith, *Angew. Chem. Int. Ed.*, 2012, **51**, 6572-6581.
5. A. Barnard, P. Posocco, M. Fermeglia, A. Tschiche, M. Calderon, S. Pricl and D. K. Smith, *Org. Biomol. Chem.*, 2014, **12**, 446-455.

View Article Online
DOI: 10.1039/C5NJ03173G

6. B. N. S. Thota, H. v. Berlepsch, C. Bottcher and R. Haag, *Chem. Commun.*, 2015, **51**, 8648-8651.
7. K. Kono, R. Ikeda, K. Tsukamoto, E. Yuba, C. Kojima and A. Harada, *Bioconjugate Chem.*, 2012, **23**, 871-879.
8. T. Yu, X. Liu, A.-L. Bolcato-Bellemin, Y. Wang, C. Liu, P. Erbacher, F. Qu, P. Rocchi, J.-P. Behr and L. Peng, *Angew. Chem. Int. Ed.*, 2012, **51**, 8478-8484.
9. E. Yuba, Y. Nakajima, K. Tsukamoto, S. Iwashita, C. Kojima, A. Harada and K. Kono, *J. Controlled Release*, 2012, **160**, 552-560.
10. X. Liu, C. Liu, J. Zhou, C. Chen, F. Qu, J. J. Rossi, P. Rocchi and L. Peng, *Nanoscale*, 2015, **7**, 3867-3875.
11. A. Barnard, P. Posocco, S. Pricl, M. Calderon, R. Haag, M. E. Hwang, V. W. T. Shum, D. W. Pack and D. K. Smith, *J. Am. Chem. Soc.*, 2011, **133**, 20288-20300.
12. B. Draghici and M. A. Ilies, *J. Med. Chem.*, 2015, **58**, 4091-4130.
13. S. Bhatia and R. Haag, in *Targeted Drug Delivery : Concepts and Design*, eds. P. V. Devarajan and S. Jain, Springer International Publishing, 2015, pp. 543-569.
14. M. R. Molla, P. Rangadurai, G. M. Pavan and S. Thayumanavan, *Nanoscale*, 2015, **7**, 3817-3837.
15. R.-S. Lee, S.-W. Wang, Y.-C. Li and J.-Y. Fang, *RSC Adv.*, 2015, **5**, 497-512.
16. Z. Jiang, H. Li, Y. You, X. Wu, S. Shao and Q. Gu, *J. Biomed. Mater. Res. A*, 2015, **103**, 65-70.
17. S. Shah, P. K. Sasmal and K.-B. Lee, *J. Mater. Chem. B*, 2014, **2**, 7685-7693.
18. Q. Jin, Y. Wang, T. Cai, H. Wang and J. Ji, *Polymer*, 2014, **55**, 4641-4650.
19. Q. Huang, T. Liu, C. Bao, Q. Lin, M. Ma and L. Zhu, *J. Mater. Chem. B*, 2014, **2**, 3333-3339.
20. L. L. Fedoryshin, A. J. Tavares, E. Petryayeva, S. Doughan and U. J. Krull, *ACS Appl. Mater. Interfaces*, 2014, **6**, 13600-13606.
21. H. Zhao, E. S. Sterner, E. B. Coughlin and P. Theato, *Macromolecules*, 2012, **45**, 1723-1736.
22. S. K. Choi, M. Verma, J. Silpe, R. E. Moody, K. Tang, J. J. Hanson and J. R. Baker, *Biorg. Med. Chem.*, 2012, **20**, 1281-1290.
23. S. K. Choi, T. Thomas, M.-H. Li, A. Kotlyar, A. Desai and J. R. Baker, *Chem. Commun.*, 2010, **46**, 2632-2634.
24. C. Bao, L. Zhu, Q. Lin and H. Tian, *Adv. Mater.*, 2015, **27**, 1647-1662.
25. M. S. Kim and S. L. Diamond, *Bioorg. Med. Chem. Lett.*, 2006, **16**, 4007-4010.
26. J. Liu, C. Detrembleur, S. Mornet, C. Jerome and E. Duguet, *J. Mater. Chem. B*, 2015, **3**, 6117-6147.
27. A. Y.-T. Huang, C.-H. Tsai, H.-Y. Chen, H.-T. Chen, C.-Y. Lu, Y.-T. Lin and C.-L. Kao, *Chem. Commun.*, 2013, **49**, 5784-5786.
28. C.-H. Hung, W.-W. Chang, S.-C. Liu, S.-J. Wu, C.-C. Chu, Y.-J. Tsai and T. Imae, *J. Biomed. Mater. Res. A*, 2015, **103**, 1595-1604.
29. H. Mizuta, S. Watanabe, Y. Sakurai, K. Nishiyama, T. Furuta, Y. Kobayashi and M. Iwamura, *Biorg. Med. Chem.*, 2002, **10**, 675-683.
30. D. A. Tomalia, *New J. Chem.*, 2012, **36**, 264-281.
31. P. Greenspan, E. P. Mayer and S. D. Fowler, *J. Cell Biol.*, 1985, **100**, 965-973.
32. J. E. T. Corrie, A. Barth, V. R. N. Munasinghe, D. R. Trentham and M. C. Hutter, *J. Am. Chem. Soc.*, 2003, **125**, 8546-8554.
33. W. Fischer, M. A. Quadir, A. Barnard, D. K. Smith and R. Haag, *Macromol. Biosci.*, 2011, **11**, 1736-1746.
34. C. Ramaswamy, T. Sakthivel, A. F. Wilderspin and A. T. Florence, *Int. J. Pharm.*, 2003, **254**, 17-21.

View Article Online
DOI: 10.1039/C5NJ03173G

View Article Online
DOI: 10.1039/C5NJ03173G

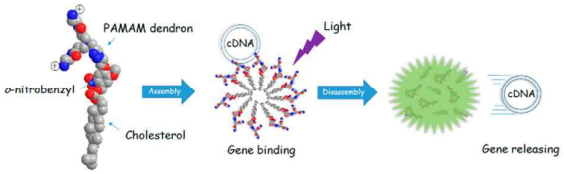

Photoresponsive amphiphilic dendron bearing a photolabile *o*-nitrobenzyl group possesses self-assembly, DNA binding and photo-induced releasing.